Available online at www.sciencedirect.com
ScienceDirect
Journal of Power Sources 158 (2006) 1054–1061
JOURNAL OF POWER SOURCES
www.elsevier.com/locate/jpowsour

# Investigation of the porous structure of battery separators using various porometric methods

A. Gigova *

*Institute of Electrochemistry and Energy Systems, Bulgarian Academy of Sciences, Sofia 1113, Bulgaria*

Available online 7 December 2005

**Abstract**

The aim of the investigation is to determine and compare the basic characteristics of the pores in battery separators using *mercury porosimetry*, which measures the volume of mercury penetrating into the pores, *capillary flow porometry*, which measures the flow rate passing through the pores, and *scanning electron microscopy*. Two groups of separators are investigated: PVC and glass mat.Two types of each group are analysed: PVC-R and PVC-E supplied by different manufacturers; and AGM and MAGM (modified AGM—new product developed by LABD at IEES).

It has been established that: the PVC-R and PVC-E separators have similar porous structures; the AGM separator and MAGM separator have different pore size distribution, as clearly evidenced by the flow porometry data; though the glass mat separators have greater total pore volume (respective porosity), the PVC separators are characterized by greater permeability, because the pores in their narrowest part have greater diameters than those for the glass mat separators. The two methods used, mercury porosimetry and capillary flow porometry, give information about different characteristics of the porous structure. A combination of both methods will provide a more detailed information about the porous structure of the separators and a clearer idea about the dynamics of the processes that take place in the lead-acid batteries, than the data supplied by each of the techniques used alone.



*Keywords:* Porous structure; Battery separators; Pore diameter; Pore volume; Pore distribution; Permeability

## 1. Introduction

The aim of porometric methods as an analytical tool is to determine the basic characteristics of porous materials, including pore volume and surface area, pore size and shape as well as pore size distribution. These parameters serve as characteristic features identifying the various porous structures, and their comparative quantitative analysis allows users to predict the properties and performance of the respective materials as well as to control the processes that take place in them [1].

Battery separators are sheets of porous materials. The porous structure of the separator allows it to be filled with electrolyte, thus ensuring the transfer of ions between the opposite electrodes during the processes of battery charge and discharge. Many authors characterize the properties of battery separators in relation to their porous structure. Zguris [2] has performed numerous investigations and tests of glass mat separators for valve regulated lead-acid batteries (VRLAB), Ball et al. [3] characterize the properties—macroscopic structure, permeability, wicking rate and diffusion of glass separators, that are most influential to VRLAB performance. Jena and Gupta [4] characterize the in-plane and through-plane pore structure of battery separators of fibrous material, and determine the effects of compression on the in-plane. Brilmyer [5] describes how the design features of a battery separator (material composition, porosity, permeability, backweb thickness) may be used to affect the performance and life of the traction lead-acid battery. Ferreira [6] investigates oxygen permeability of PVC separators through dry separator materials and partly saturated materials.

Permeability, stability, strength and maximum ion conductivity are basic characteristics of the separators. Therefore, investigation and control of their porous structure are very important factors for proper functioning of the batteries.

The objective of the present investigation is to determine the basic characteristics of the pores in two types of battery separators using different porometric methods.

## 2. Experimental

Two techniques are used in the present work: mercury porosimetry and capillary flow porometry. The principle of

* Tel.: +359 2 9792719; fax: +359 2 8731552.
*E-mail address:* adrianag@mail.bg.

0378-7753/$ – see front matter © 2005 Elsevier B.V. All rights reserved.
doi:10.1016/j.jpowsour.2005.11.006

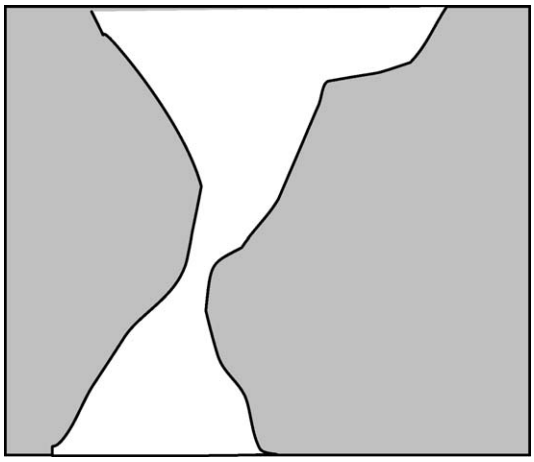

Fig. 1. Variation in pore cross-section along pore length.

operation of both methods is based on the physical principle of penetration of liquids into small cylindrical pores, i.e. the theory of capillary phenomena, which can be represented by the Washburn equation [1,7]:

$$D = \pm\frac{4\sigma\ \cos\theta}{P} \quad (1)$$

where $D$ is the diameter of the pore assuming that it is cylindrical; $P$ the applied pressure; $\sigma$ the surface tension of the liquid that penetrates into the pores; and $\theta$ the contact angle of this liquid.

Pores are seldom cylindrical. Hence, the above equation refers to a special model that may not reflect accurately the pore structure of the actual materials. However, its application has been adopted as a practical tool for characterizing a fairly complex problem. Most often the cross-section of a given pore varies along its length (Fig. 1). That is why pore size measurements carried out by different methods may yield different results [1,7].

### 2.1. Mercury porosimetry

In this method, the previously weighed sample from the separator is evacuated and then filled with mercury. The direct measurement of the volume of mercury penetrating into the pores of the separator sample at an applied external pressure gives the pore volume and the pore volume distribution by size. The porosity (%), total pore area, median pore diameter, and bulk density of the separator can be calculated from the pore volume [1].

The main drawback of this method is the application of high pressures, which may compress the separator samples and hence yield inaccurate results.

A MICROMERITICS AutoPore 9200 instrument was used in our investigations.

### 2.2. Capillary flow porometry

In this method, the sample from the separator is soaked with a wetting liquid and gas pressure is applied on one side of the sample. The gas pressure is increased slowly until the liquid is removed from the pores and a gas flow forms, which then increases with further increase in pressure [4,7]. The flow rate as a function of gas pressure is measured experimentally and gives the diameter of each pore in its narrowest part. Permeability, largest pore diameter, mean flow pore diameter and pore size distribution can be measured with this method.

In our tests, we used alcohol and porewick$^{TM}$ as wetting liquid. We measured the permeability of dry separator samples. The gas pressure applied was 28 kPa. A PMI Capillary Flow Porometer was used for these measurements.

The results of the porometric measurements were compared with the observations of the separator structure by scanning electron microscopy (JEOL JEM 200Cx microscope). By this latter method we obtained direct information about the porous structure of the separator samples and about the size, shape and interconnection of the pores at the surface of the samples.

Two types of separators were investigated: PVC and glass mat. The PVC separator samples, supplied by different manufacturers, were for starter and traction lead-acid batteries. These samples are designated as PVC-R and PVC-E.

The glass mat samples were: absorptive glass mat (AGM) and modified absorptive glass mat (MAGM) separators. MAGM is a new product developed by the research team of the LABD at IEES [8,9]. This is AGM separator whose two surfaces are treated with polymeric emulsions of different concentrations. These separators are assembled in valve-regulated lead-acid batteries. The two glass mat separator samples are designated as AGM and MAGM.

In order to facilitate the comparison of all separators under test, the backweb thickness of all separator samples was measured. The obtained results are: 0.6 mm for PVC-R, 0.7 mm for PVC-E, 2.9 mm for AGM and 2.8 mm for MAGM, respectively.

## 3. Results and discussion

### 3.1. Separator structure determined by scanning electron microscopy

Fig. 2 presents SEM pictures of the PVC-R and PVC-E separator samples. These separators comprise thermally sintered PVC particles that form a porous mass. Both separators have similar structure. Pores sized 10.5, 18.5 and 21 μm are measured from the pictures.

Fig. 3 shows SEM pictures of AGM and MAGM separator samples. While the AGM separator is built of non-interconnected glass fibers of various thickness forming pores of various size in between, the glass fibers in the MAGM sample are interconnected through the polymeric emulsion forming a continuous porous mass. When immersed in water or in $H_2SO_4$ solution, the AGM separator disintegrates into individual fibers, whereas the MAGM sample preserves its structure unchanged. As evident from the pictures, the structure of the glass mat separators does not allow for measuring the pore sizes.

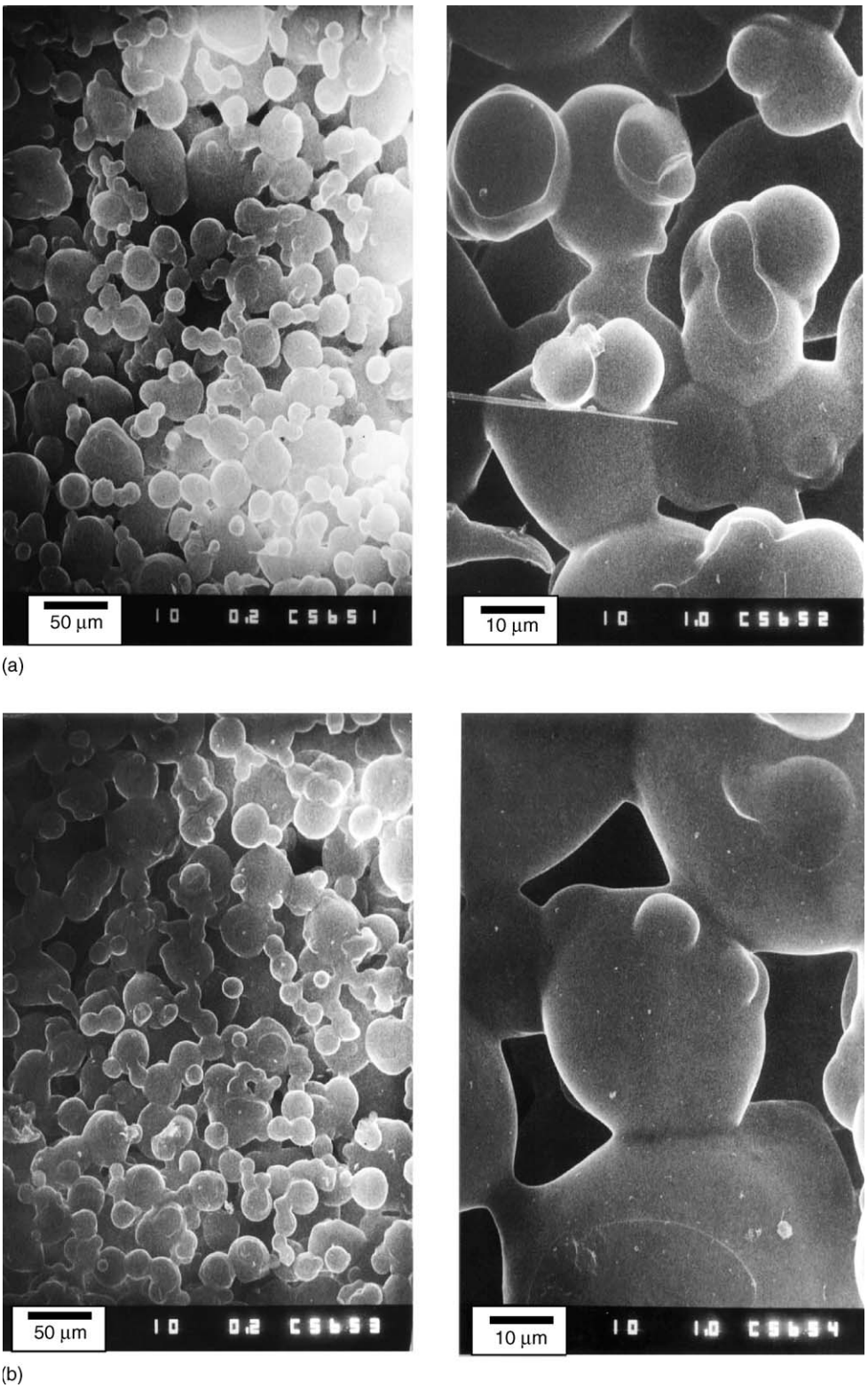


Fig. 2. SEM micrographs of the structure of PVC-R (a) and PVC-E (b) separators at two magnifications.

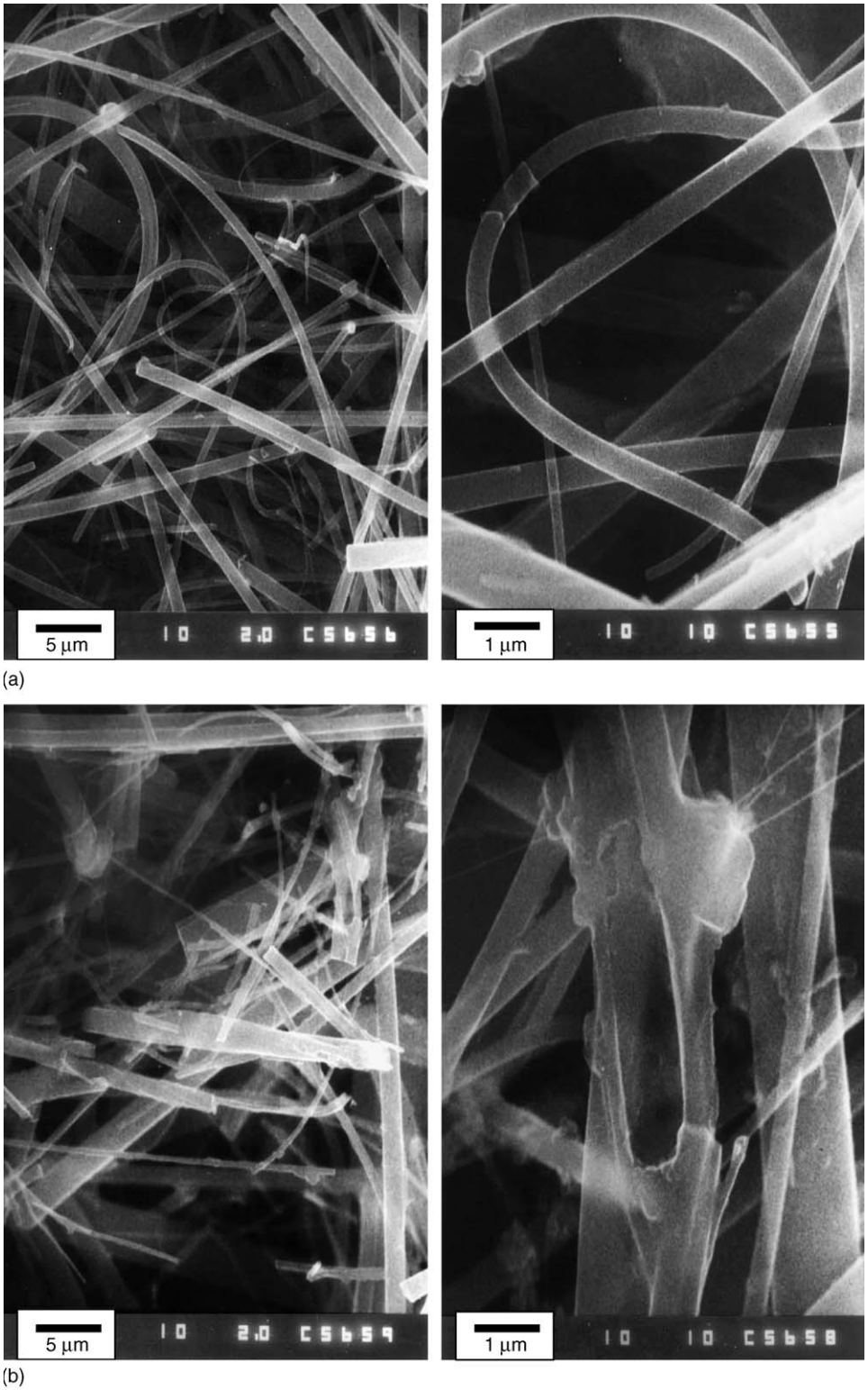


Fig. 3. SEM micrographs of the structure of AGM (a) and MAGM (b) separators at two magnifications.

Table 1

| Characteristics | PVC-R | PVC-E | AGM | MAGM |
|---|---|---|---|---|
| Total pore volume ($cm^3\ g^{-1}$) | 0.372 | 0.355 | 3.293 | 2.845 |
| Porosity (%) | 35.34 | 33.95 | 55.36 | 52.33 |
| Total pore area ($m^2\ g^{-1}$) | 8.539 | 9.870 | 1.341 | 1.335 |
| Median pore diameter (volume) (μm) | 19.827 | 19.118 | 21.026 | 23.424 |
| Bulk density ($g\ cm^{-3}$) | 0.946 | 0.957 | 0.168 | 0.184 |

### 3.2. Pore volume and pore volume distribution determined through mercury porosimetry

#### 3.2.1. Total pore volume, porosity, total pore area and bulk density

The maximum volume of mercury that intrudes into the pores of the separator sample at maximum applied working pressure gives the total pore volume. The porosity of the sample gives the percent share of these pores in the sample volume. The total pore area is the surface area of the pore walls under maximum applied pressure [1].

The basic characteristics of the separator samples determined by the method of mercury porosimetry are summarized in Table 1.

The data in table give grounds for the following conclusions:

(a) The total pore volumes of the two PVC separator samples are very close, that of the PVC-R sample being larger than that of the PVC-E sample by only 4.8%. Hence, the percent porosity of the PVC-R separator is a bit higher than the porosity of the PVC-E sample. This small difference in porosity results in a slightly greater bulk density of the PVC-E separator and a smaller median pore diameter of its pores as compared to its PVC-R counterpart. The total pore surface area of the PVC-R separator is smaller than that of the PVC-E sample by 13.48%. The minor differences between the pore characteristics of the two types of PVC separators as well as the similarity in their structure evidenced by the scanning electron microscopy examinations indicate that, most probably, the two manufacturers have used PVC powder supplied by the same source and the small differences in separator properties are due to differences in the technology of the sintering process used.

(b) The total pore volume of the AGM separator is greater than that of the MAGM sample. As a result of the treatment of AGM separator with the polymeric emulsion, its pore volume has decreased by 13.62%, whereas the pore surface area has diminished by 0.5% only. The porosity of the polymer-treated MAGM sample is smaller than that of the untreated AGM by 5.5%, but the median pore diameter of the MAGM sample is by ca. 11% larger than that of the AGM separator. It can be assumed that the polymeric emulsion causes the volume of the obtained MAGM separator to shrink under the action of the disjoining pressure created on concentration of the polymeric emulsion at the sites of contact between the glass fibers. This happens during the thermal treatment of MAGM and leads to a 9.52% increase in bulk density of the MAGM separator as compared to its AGM counterpart.

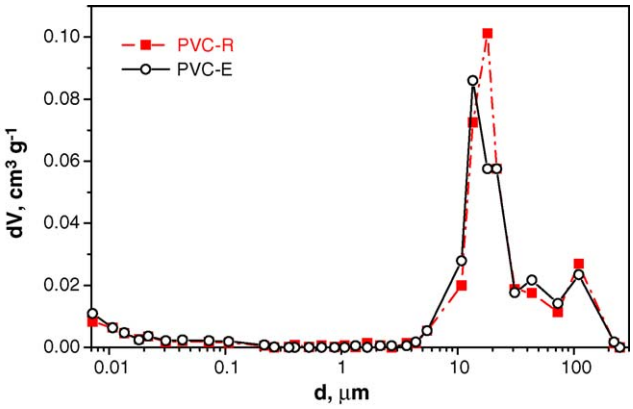


Fig. 4. Pore volume distrubution for PVC separators.

(c) A comparison between the data for the two types of separators shows that the glass mat separators have greater total pore volume, porosity and median pore diameter (volume), but smaller bulk density and total pore area than the PVC separators. These results indicate that the glass mat separators contain more electrolyte and hence the flow of ions ($H^+$ and $SO^{2-}$) through them will be less impeded than that through the PVC separators.

#### 3.2.2. Pore volume distribution by pore diameter

Fig. 4 presents the differential pore volume distribution curves versus pore diameter for the two types of PVC separators. Fig. 5 shows analogous pore distribution plots for the AGM and MAGM separator samples.

The differential pore volume distribution curves indicate that the PVC separators contain pores within a wide range of diameters between 0.007 and 0.1 μm, and between 4 and 200 μm, whereas the pores formed between the glass fibers are large in volume: between 5 and 200 μm. The maximum peak in the differential curves for glass mat separators decreases on treating the separator with polymeric emulsion, with no substantial change in the diameter at which it appears, 11 μm (Fig. 5). In the case of the PVC separator samples, the maximum peak in the differential curves occurs at 18.0 μm for PVC-R and at 13.5 μm for PVC-E, respectively (Fig. 4).

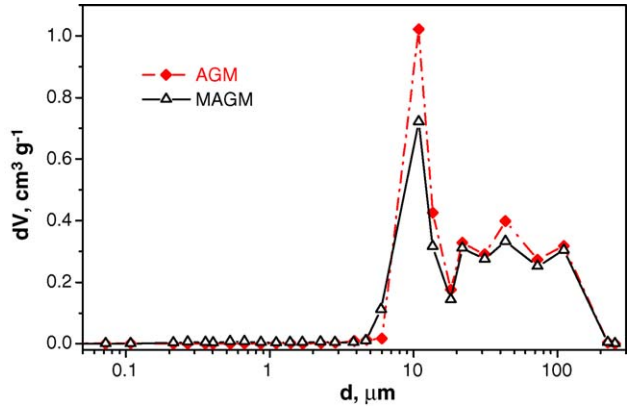


Fig. 5. Pore volume distribution for AGM and MAGM separators.

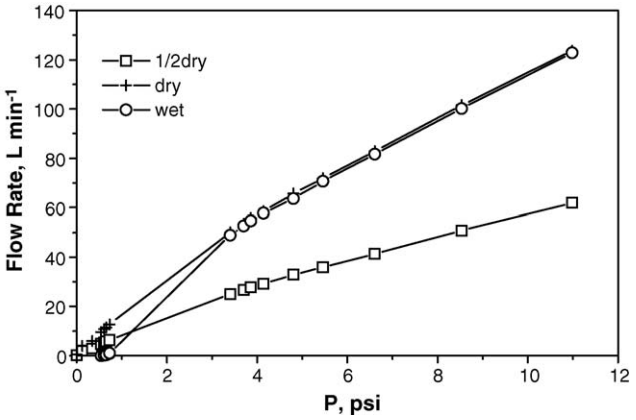


Fig. 6. Typical flow porometry curves for PVC-E separator.

Judging by the profile of these curves, the pore volume distribution for each separator sample comprises two zones of pore sizes:

- *Micro pores*: up to 30 μm for PVC and up to 20 μm for glass mat separators. These are the pores that constitute the maximum share of the total pore volume.
- *Macro pores*: from 30 to 200 μm for PVC separators and from 20 to 200 μm for glass mat separators. The volume of the pores belonging to this region is about 10 times larger in the glass mat than in the PVC separators. It can be assumed that the oxygen flows travel mainly through the macro pores in the glass mat separators, whereas the ion and water flows pass predominantly through the micro pores. The relatively large number of macro pores in the glass mat separators facilitates the transfer of oxygen flows from the positive to the negative plates.

### *3.3. Separator permeability and pore size distribution determined by capillary flow porometry*

#### *3.3.1. Largest, mean and smallest pore diameter and permeability*

The typical curves obtained by capillary flow porometry measurements on the PVC-E separator sample are presented in Fig. 6. Similar curves are also plotted for each separator under test and these curves provide the following information. "Dry" and "wet" curves correspond to dry and wet samples, respectively. The "half-dry" curve is calculated from the "dry" curve and gives half the flow rate at a given pressure. The pressure at which the flow starts is known as "bubble point pressure". This is the minimum pressure required for a gas bubble to penetrate through the pores of the sample filled with liquid. This pressure corresponds to the largest pore diameter. The intersection of the "half-dry" curve with the "wet" curve gives the pressure corresponding to the mean flow pore diameter. Also, the "dry" curve gives the permeability of air through the separator [4,7].

Table 2 presents the basic pore characteristics determined by capillary flow porometry for the separators under test.

(a) The PVC-E separator has greater diameter of the largest pores, but smaller diameters of mean and smallest pores than these of PVC-R sample. At the same time, the permeability of PVC-R is higher by almost 10% than that of PVC-E. This implies that the pores with the largest diameter have weaker effect than those with mean and smallest diameters. This conclusion is also confirmed by the mercury porosimetry data: the separator with higher permeability, PVC-R, has total pore volume greater than that of the PVC-E sample.

(b) The largest pore diameter measured for the MAGM sample is smaller than that for the AGM sample because these pores in the MAGM separator are partially filled with polymeric emulsion. The MAGM separator has greater mean flow pore diameter (by 23%) and greater diameter of the smallest detected pore (by 7%) as compared to those for AGM. The permeability of the MAGM separator is a bit higher (by 3%) than that of the AGM sample. These results indicate that the treatment of AGM with polymeric emulsiom, though reducing the total pore volume (Table 1) and the largest pore diameter (Table 2), improves slightly the permeability of MAGM as compared to that of the untreated AGM separator. This is probably due to the fact that the emulsion shapes the pore channels (the wall of the pore channel becomes smoother), thus improving the permeability of the MAGM separator.

*Flow porometry measurements using different wetting liquids.* Glass mat separators have a fragile skeleton structure. AGM and MAGM samples were tested using different wetting liquids (with different surface tensions, $\sigma$) and the obtained results are summarized in Table 3.

The results indicate that when alcohol is used as a wetting liquid, the measured diameter values are larger than when the samples are wetted with porewick$^{TM}$.

(c) The largest pores in the PVC separators are a little bit greater in diameter compared to those in glass mat separators. But the difference between the mean flow pore diameter, as well as between the smallest detected diameter for PVC and glass mat separators is more than three times. Due to the larger size

Table 2

| Sample | Diameter (μm) | | | | Permeability (l min$^{-1}$ cm$^{-2}$) |
|---|---|---|---|---|---|
| | Largest pore | Mean flow pore | Smallest detected pore | At maximum pore distribution | |
| PVC-R | 16.378 | 10.568 | 9.021 | 9.021 | 20.12 |
| PVC-E | 17.524 | 10.353 | 8.432 | 8.432 | 18.25 |
| AGM | 14.953 | 3.061 | 2.091 | 2.704 | 6.39 |
| MAGM | 14.235 | 3.764 | 2.241 | 3.746 | 6.58 |

Table 3

| Sample | Diameter (μm) | |
|---|---|---|
| | Largest pore | At maximum pore distribution |
| | Test I. Alcohol $\sigma = 22.3\,\text{dyn cm}^{-1}$ | |
| AGM | 14.953 | 2.704 |
| MAGM | 14.235 | 3.746 |
| | Test II. Porewick™ $\sigma = 16.0\,\text{dyn cm}^{-1}$ | |
| AGM | 10.553 | 1.877 |
| MAGM | 10.185 | 2.291 |

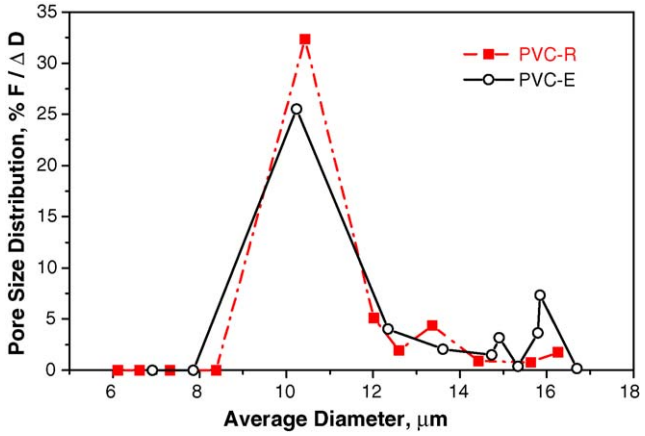


Fig. 7. Pore size distribution for PVC separators.

of the pores in PVC separators, their permeability is three times higher than that of glass mat separators. Moreover, the thickness of PVC separators is about four times smaller than that of glass mat separators.

### 3.3.2. *Pore size distribution by diameter*

The percentage flow of gas (*%F*) passing through pores having diameters within narrow specified ranges was calculated from the experimental data. The PMI technique [4,7] was employed and the obtained results are present in Figs. 7–9 as plots of [*%F*/Δ*D*] versus [average *D*]. These plots are referred to as pore size distribution.

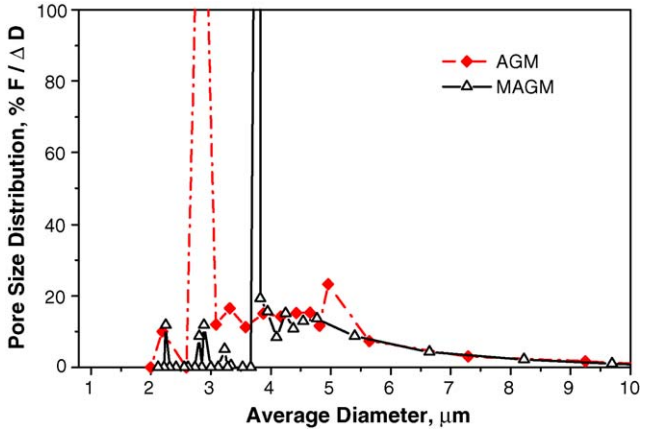


Fig. 8. Pore size distribution for glass mat separators tested with alcohol, $\sigma = 22.3\,\text{dyn cm}^{-1}$.

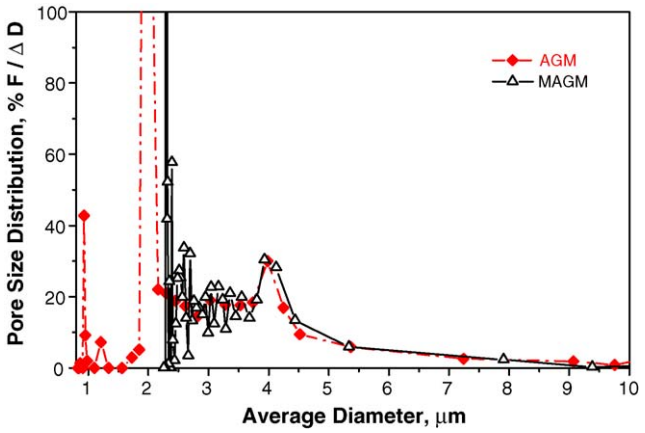


Fig. 9. Pore size distribution for glass mat separators tested with PoreWick™, $\sigma = 16\,\text{dyn cm}^{-1}$.

The pore size distribution by diameter obtained for the PVC separator samples is presented in Fig. 7. The peak in the distribution curves for both PVC samples occurs at pore diameters between 10 and 11 μm.

Figs. 8 and 9 give the pore size distribution curves for the AGM and MAGM samples, determined using different wetting liquids. These curves show interesting findings and they differ from one another. Test I (wetting liquid with $\sigma = 22.3\,\text{dyn cm}^{-1}$) yields a peak in the pore size distribution curves at about 2.70 μm for AGM and 3.75 μm for MAGM, respectively. Test II (wetting liquid with $\sigma = 16.0\,\text{dyn cm}^{-1}$) registers the peaks in the pore size distribution curves at about 1.88 μm for AGM and at 2.29 μm for MAGM. The pore sizes measured during test II decrease proportionally as compared to those measured during test I for both AGM and MAGM separators. This is due to the fact that the wetting liquid used in the second test has lower surface tension and hence the capillary resistance when the liquid is displaced by the gas flow from the pores of the glass mat separators is lower. As evident from the figure, the peak in the pore size distribution curve for MAGM shifts to larger pore diameters, it has high intensity and is narrow. The peak in the AGM distribution curve is broader, which means that the pores in the AGM separator vary within a wider range of sizes. This finding is supported by the results of the two tests using two different wetting liquids. The AGM separator is a combination of glass fibers of different thickness, forming pores with larger or smaller diameters between the fibers. The polymeric emulsion "glues" several thin glass fibers into a single thicker fiber and thus creates (opens) new larger pores. It can be assumed that the largest pores in the AGM separator decrease in size after the treatment with the emulsion and some of the smaller pores are plugged altogether. All above processes are responsible for the re-distribution of the pores, i.e. for the formation of a new porous structure of more uniform pore distribution by diameter, in the MAGM separator.

The obtained pore size distribution curves for the AGM and MAGM separator samples are different because the polymeric emulsion has changed substantially the porous structure of the MAGM separator. So, the porometric measurements indicate that the number and size of the pores, and their distribution by

size are strongly affected by the polymer, whose structure and properties yield a new product (MAGM) with specific features and behaviour.

### *3.4. Comparison between the porous structures of the separators determined by mercury porosimetry and capillary flow porometry*

#### *3.4.1. Mean pore diameter*

The mean pore diameter can be measured by the two methods and the obtained results are summarized in Tables 1 and 2. The median pore diameter (volume) measured by mercury porosimerty is about twice greater than the mean flow pore diameter measured by flow porometry for the PVC separators. There is a seven-fold difference in mean pore diameter as measured by the two methods for the AGM separators, this difference being reduced to six times for the MAGM sample. The above results imply that the pores have wide mouths as those illustrated in Fig. 1, which is most pronounced with glass mat separators. Pores of complex shapes form between the glass fibers, whereas the pores formed between the PVC grains are closer to cylindrical shapes. These findings support the conclusion drawn earlier that the polymeric emulsion shapes the pore channels in MAGM separators.

#### *3.4.2. Pore size distribution*

The pore size distribution data obtained by mercury porosimetry and flow porometry differ substantially for one and the same material. Porosimetry measures large pores of substantial volumes, whereas flow porometry evidences small pores. These results can be explained by the shape of the pore presented in Fig. 1. The pore has a constricted part, but a wide mouth. This pore will be detected by flow porometry as a single pore of small diameter. Mercury porosimetry will measure the wider parts of the pore as large pores of considerable volume and the narrowest part as a small pore of small volume.

A comparison between the pore size distribution curves for the different separators (Figs. 4, 5, 7, 8 and 9) shows that the pore diameters determined by capillary flow porometry are several times smaller than those determined by mercury porosimetry. This difference is a result of two factors. On the one hand, capillary flow porometry measures not the pore volume, but rather the pore diameter in the narrowest part of the pores, disregarding their complex shape and cross-section. The second reason for the different results obtained is the application of high pressure in the case of mercury porosimetry. As separators are made of soft material with an unstable skeleton structure (especially glass mat separators), the mercury intruded into the sample causes the pore volume to "swell" and hence a larger pore diameter is registered.

## 4. Summary

1. Two groups of battery separators (two types of each group) have been investigated: PVC and glass mat. It has been established that:
   - the PVC-R and PVC-E separators have similar porous structures;
   - the AGM separator and the modified AGM (MAGM) separator have different pore size distribution, as clearly evidenced by the capillary flow porometry data;
   - though the glass mat separators have greater total pore volume (respective porosity), the PVC separators are characterized by greater permeability, because the pores in their narrowest part have greater diameters than those in the glass mat separators.
2. The two methods used: *mercury porosimetry* and *capillary flow porometry* give information about different characteristics of the porous structure. A combination of both methods will provide a more detailed information about the porous structure of the separators and a clearer idea about the dynamics of the processes that take place in the lead-acid batteries, than the data supplied by each of the techniques used alone.

## Acknowledgement

The author extends her sincere gratitude to Prof. D. Pavlov and Dr. G. Papazov for their valuable help and most useful comments and advice when conducting this work.

## References

[1] T.G. Plachenov, S.D. Kolosentsev, Porometria, "Khimia", Leningrad, 1988 (in Russian).
[2] G.C. Zguris, J. Power Sources 73 (1998) 60.
[3] R.J. Ball, R. Evans, R. Stevens, J. Power Sources 104 (2002) 208.
[4] A.K. Jena, K.M. Gupta, J. Power Sources 80 (1999) 46.
[5] G.H. Brilmyer, J. Power Sources 78 (1999) 68.
[6] A.L. Ferreira, in: Proceedings of the LABAT'96 Conference, Varna, Bulgaria, 1996, p. 142 (abstract no. 41).
[7] A. Jena, K. Gupta, Fluid Particle Sep. J. 14 (3) (2002) 227.
[8] D. Pavlov, S. Ruevski, V. Naidenov, G. Sheitanov, J. Power Sources 85 (2000) 164.
[9] D. Pavlov, V. Naidenov, S. Ruevski, V. Mircheva, M. Cherneva, J. Power Sources 113 (2003) 209.